Chem. Senses 26: 1005–1013, 2001

Orbital Response Indicates Nasal Pungency: Analysis of Biomechanical Strain on the Skin

Alfredo A. Jalowayski[1,2], Bradley N. Johnson[1,3], Paul M. Wise[1], Geert W. Schmid-Schönbein[3] and William S. Cain[1]

[1]Chemosensory Perception Laboratory, Department of Surgery (Otolaryngology), [2]Department of Pediatrics and [3]Department of Bioengineering, University of California, San Diego, La Jolla, California, USA

Correspondence to be sent to: Alfredo A. Jalowayski, Chemosensory Perception Laboratory, Mail Code 0957, University of California, San Diego, La Jolla, CA 92093-0957, USA. e-mail: ajaloway@ucsd.edu

Abstract

Stimulation of the human nasal passage with pungent vapor elicits motor responses in a zone around the eye. This investigation addressed whether quantification of such responses, particularly activity of the orbicularis oculi muscle, could yield a sensitive index of nasal pungency. We placed an array of small, high-contrast targets just beneath the lower eyelid and videotaped their movement to capture deformation of the skin atop the orbicularis oculi during 3 s stimulation with pungent concentrations of ethyl acetate. Eleven subjects participated. Analysis of the movements served to determine mechanical strain, which yielded a single index that we termed 'maximum strain'. This increased with concentration of the vapor and with time during and just after stimulation. Comparison with psychophysical data showed that the strain became evident at concentrations just detectable as pungent. Maximum strain measured on the skin shows promise as an objective index of pungency.

Introduction

The trigeminal nerve, which mediates somesthesis in the face, eyes, nasal passages and anterior oral cavity, serves as the afferent limb of many reflexes, some little understood (Widdicome, 1961). The responses include some evoked by chemesthetic stimulation, particularly pungent or irritating stimulation. An irritating vapor at the eye, for example, may precipitate blinking and tearing. An irritating vapor in the nasal passage may increase mucus flow and, if strong enough, cause momentary apnea.

Virtually everyone has experienced how a whiff of smelling salts can take the breath away for an instant. Cain and associates (Cometto-Muñiz and Cain, 1982, 1984; Dunn *et al*., 1982; Garcia-Medina and Cain, 1982; Stevens and Cain, 1986) established that the threshold for the apneic response fell into register with perceived pungency. For example, the threshold followed the same time-intensity trading as perceived pungency; it lay higher in smokers than in non-smokers, in accordance with perceived pungency, which smokers found less intense than did non-smokers; it lay higher in males than in females, again in accordance with perceived nasal pungency; it lay higher in older than in younger persons, also in accordance with perceived pungency; and it summed across the two nasal passages in the same way as perceived pungency.

These findings indicated that the apneic response possesses some potential as an objective index of nasal irritation. A good index would have the potential to bypass often tedious psychophysical testing over many trials to indicate the state of sensitivity of a person or group and would provide a continuum of response from around threshold to suprathreshold levels of stimulation. As such an index, the apneic reaction has the disadvantage that it occurs only at high levels of stimulation. That is, although the threshold for the reaction correlates (negatively) with relative chemesthetic magnitude, it does not itself indicate the concentration where pungency begins to occur. It may also have too much variability to serve as a faithful index for individual subjects (Shusterman and Balmes, 1997). The variability arises at least in part from the superposition of the response on an already dynamic event. That is, it essentially rides atop and modulates the already changing contractions of the diaphragm as a person inhales or exhales.

Videotapes of the faces of subjects in experiments on the apneic reaction revealed small twitches of the orbicularis oculi at levels of stimulation below that necessary to trigger apnea. As level of stimulation increased, the twitches became more pronounced and widespread in the orbital area, culminating at high levels in squinting and blinking.

(At lower levels, stimulation of one nostril leads to ipsilateral activation, whereas at higher levels, it leads to bilateral activation.) If quantifiable, the response seemed a potential replacement for the apneic response as an objective index. During normal breathing, the orbicularis oculi undergoes no systematic contraction, so that its twitches could appear against an otherwise static background. Furthermore, the response could occur even without active inhalation of a stimulus, but just passive flow into the nostril while breathing takes place via the mouth.

Initial efforts to quantify orbital reactions applied a variant of the Facial Action Coding System (FACS) of Ekman and associates (Ekman and Friesen, 1975; Ekman and Rosenberg, 1997). Analysis of the reactions on videotape led to a scheme of nine relevant actions (raising eyebrow, blinking, lower lid twitching, etc.). Trained judges rated the individual components on a scale of 0–4. This involved laborious scoring frame-by-frame and of course had some subjective component. Inter-judge reliability lay in the vicinity of 0.7–0.8, too low in view of the hours of effort required to score just one test session.

The search for an alternative led to examination of quantitative measurement of mechanical strains on biological surfaces. Simon and Schmid-Schönbein (Simon and Schmid-Schönbein, 1990), for example, developed methods for quantitative measurement of mechanical strains in the cytoplasm of individual cells. McCulloch and colleagues (McCulloch *et al*., 1998; Mazhari *et al*., 1998) used similar methods to measure strains in the myocardium. The methodology has included video-analysis of arrays of small targets attached to tissue and computation of non-linear mechanical Lagrangian strains (change of length per unit initial length) and principal strains (Fung, 1994). The present report summarizes efforts to apply such methodology to quantify the orbital response. The work relied upon video-recording of small markers on the skin below the lower lid and computation of the Lagrangian strains from the relative movement of the markers.

Ideally, an objective reaction to chemesthetic stimulation should have the same sensitivity as that measured psychophysically. Figure 1 depicts a surrogate function for the detectability of pungency from ethyl acetate, the test material of this study. The function incorporates results from 10 normosmic subjects who localized the source of pungent stimulation to the right or left nostril (W.S. Cain *et al*., submitted for publication). Functions for localization give equivalent information to those for detection and avoid the problem that normosmic subjects cannot make blinded judgments of detection since odor discloses the presence of the stimulus (Cometto-Muñiz and Cain, 1998). Since subjects cannot reliably localize odor to the right or left nostril but can localize pungency, even if just barely detectable, the function for localization circumvents the problem. The function in Figure 1 indicates that in a one log-unit span beginning at 3.6 log p.p.m., detection went from quite low to perfect. Consequently, the concentrations of interest in the present study lay in this range.

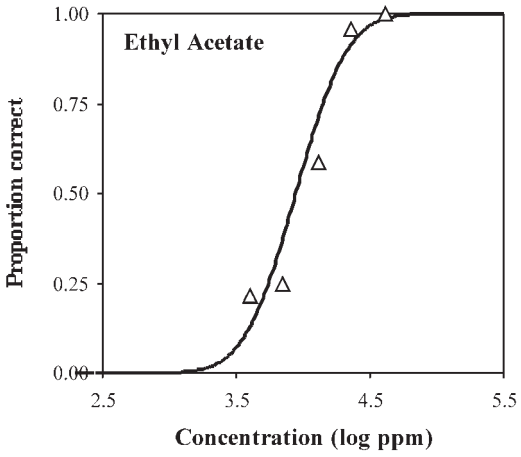

Figure 1 Psychometric function for the detection of pungency determined by localization (W.S. Cain *et al*., submitted for publication). On a trial, a subject sniffed from two vessels, one connected via a Teflon nose-piece to the right nostril and another connected similarly to the left nostril. One vessel, randomly determined on a trial, contained vapor of ethyl acetate and the other did not. The points represent the proportion of correct answers obtained from 10 young subjects, each of whom made 28 judgments per concentration (vapor phase, v/v). The curve is the best-fitting (least-squares method) cumulative Gaussian function.

Materials and methods

Subjects

Eleven screened subjects (seven males, four females; aged 21–59) participated after they provided informed consent. The protocol had approval of the Human Subjects Committee of the University of California. In screening, subjects gave relevant medical history and had a physical examination of the nasal passages. Criteria for exclusion via history principally concerned chronic or recent acute disorders of the airways or eyes. Criteria for exclusion via examination of the nose concerned deviation of the septum, chronic hypertrophic rhinitis, polyposis and signs of acute or chronic infection. Examination of the eyes and periorbital area ruled out the use of contact lenses, presence of facial paralysis, or abnormal twitching of the eyelids.

Ten subjects participated in two sessions and one in three, the first session for screening and orientation and the next for chemosensory testing. Testing lasted ~1.5 h. Subjects earned US$10 per hour.

Stimulus

Ethyl acetate (Aldrich, Milwaukee, WI, 99.8%) was the stimulus. Vapor concentrations used in testing ranged from 3.6 to 4.3 log p.p.m. (v/v), plus a blank.

Apparatus

Olfactometer

A flow-dilution olfactometer delivered controlled amounts of vapor to the right nostril at a flow rate of 6 l/min and a temperature of 36°C. Nitrogen sparged through 200 ml of liquid-phase ethyl acetate provided a continuous feed stream metered on command into a carrier stream of air humidified to 80% RH. A program in LabView controlled the dilution and timing of the stimulus. Rise-time of stimulus in the carrier stream was ~20 ms.

Injection of vapor into the carrier stream occurred virtually seamlessly by means of a switching scheme devised by Kobal (Kobal, 1985; Kobal and Hummel, 1988). Closing a solenoid valve connected to a vacuum source added stimulus (feed stream) to the carrier stream, while the simultaneous opening of another solenoid removed an amount equal to that added. Hence, if the concentration desired on a trial was 10% saturated vapor, a feed stream of 0.6 l/min entered the carrier stream for 3 s, while simultaneously 0.6 l/min of carrier stream exited for 3 s. Placement of the solenoid valves and vacuum source away from the experimental room ensured noiseless switching at the site of testing.

The experimenter calibrated concentration of the vapors off-line by means of gas–liquid chromatography (GC). Samples of vapor were taken in quintuplicate or more by gas-tight syringe at the nose-piece. (Checks for the presence of aerosol at the nose-piece revealed none.) Measurement of responses to liquid-phase ethyl acetate allowed expression of GC responses to vapor samples in terms of mass and vapor concentration. The geometric average coefficient of variation in the concentration of the vapor samples was 7.7%.

Video system

A Pulnix TM-6710 high-speed digital video camera equipped with a 55 mm Micro-Nikkor 1:2.8 lens served to track movement of high-contrast markers placed below the orbit of the right eye. The camera recorded at 60 frames/s. A PC-based microprocessor running a routine developed by Speed Vision Technologies Inc. (San Diego, CA) controlled operation of the camera. A relay circuit linked operation of the computer for the video camera to that for the olfactometer, so that the triggering signal could come from a keystroke that activated delivery of vapor for 3 s.

For video acquisition of the effects of stimulation, a trial lasted 5.7 s or 305 frames plus 30 (frames 5–35) frames that held information prior to the triggering signal. After accumulation of the relevant 340 frames, the entire buffer was written to disk as an Omni Speed Movie (OSM) file. Visible 'switches' overlain on the saved frames indicated whether they had been acquired before or after the triggering signal. The state of the trigger displayed at the 36th frame served to verify that data acquisition had occurred as expected.

Procedure

A subject began participation with a session of screening and orientation regarding procedures (e.g. application of the nose-piece). The subjects then practiced velopharyngeal closure, a technique that entails breathing through the mouth while maintaining air static in the nasal cavity. That procedure made it possible for flow from the olfactometer to enter a nostril and stimulate chemoreceptors without need for the subject to breathe the vapor.

A test session began with placement of five or six high-contrast markers just below the lower eyelid and two at the base of the bridge of the nose, as illustrated in Figure 2. The markers were black dots (0.9 mm diameter) with white rings (3 mm diameter) created in Adobe Illustrator and printed onto adhesive labels. The experimenter affixed these on the skin with fine tweezers. Placement varied somewhat

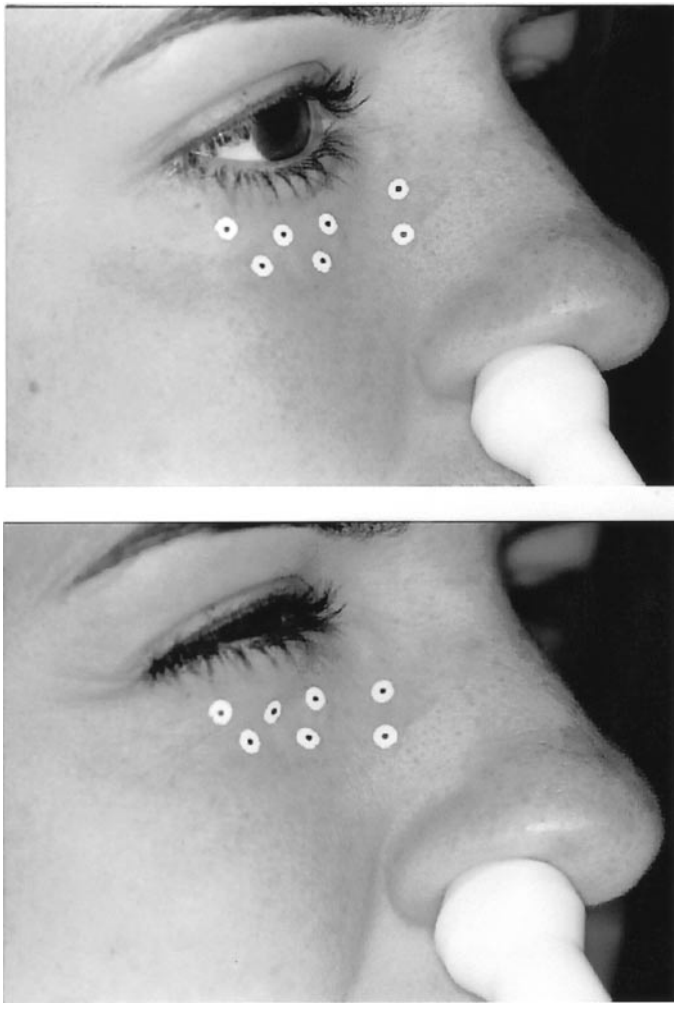

Figure 2 A subject with seven high-contrast markers on her skin, five in the responsive region below the lower lid and two alongside the bridge of the nose. The two served as the base of five potential triangles, with the other markers as apices. Top image shows positions before and bottom image shows positions after delivery of stimulus.

from subject to subject depending upon how the skin moved during blinking.

Videotaping required the subject to remain stationary during a trial. The subject sat comfortably in an adjustable chair with his/her head against a headrest. The experimenter brought the arm of the olfactometer to a position that would allow a Teflon nose-piece at the end of a short length of flexible tubing to make a seal around the nares with minimal disturbance of the nasal anatomy (Figure 2). The subject put the piece in place; this was easily accomplished with virtually no movement of the head. The nose-piece served both to deliver flow to the nostril and to vent the flow through axial channels. The camera sat a few degrees off the median plane of the subject's head, normal to the plane of motion of the markers. The field of the camera appeared as a live image on the computer monitor. A computer-controlled zoom function facilitated focusing by providing a magnified view of the markers on the face.

Trials proceeded as follows. At a ready signal, the subject put the nose-piece snugly to the naris, closed the velopharynx, leaned back against the head rest and looked straight ahead. During that period, the nose-piece delivered warmed, humidified air. The experimenter verified focus, then sent the triggering signal for noiseless delivery of vapor for 3 s. The subject remained still until the period of data acquisition ended, then removed the nose-piece and could relax for 2 min. A session generally consisted of 24 trials, six concentrations ranging from a blank to 4.3 log p.p.m. presented four times.

Image processing

For processing of the videos, the saved OSM files were converted to TIFF images analysable by a program that tracked movement of the dots via a feature-boundary extraction algorithm (written for Matlab, C Mathworks). Relative movement of the markers through a sequence of images captured deformation of the subject's skin from contraction of the orbicularis oculi.

The analyst set up a small rectangular field, called a region of interest (ROI), around each dot. Gray-scale thresholding gave an ROI two levels of gray, a white and a black. The thresholding reset the ROI sub-image so that pixels with gray values below a threshold value equaled zero (white) and those equal to or above the threshold equaled 255 (black). This procedure changed the small gray-level gradient near the boundary of the marker into a steep gradient, just one pixel wide. The black pixels then constituted the marker with its center the numerical solution of the two integrals,

$$\bar{x} = \frac{1}{A}\int_A x\mathrm{d}A \quad \bar{y} = \frac{1}{A}\int_A y\mathrm{d}A$$

where A represents area of the marker computed by counting number of black pixels. These double integrals were evaluated with a routine in the image-processing toolbox for Matlab.

Once the center of a marker was located, the ROI was centered over it and the coordinates of the center stored in memory. Then the next frame in the series was loaded and the ROI from the previous frame placed upon it. The thresholding procedure was applied to locate the x and y coordinates of the target in the second frame within the ROI. This continued until all the targets in a frame were represented as coordinates in ROIs. A filter with a window of five frames smoothed the changes in coordinates across frames. Files of the coordinates for each marker over the sequence of frames comprised the data for computation of strains.

Strain analysis

Two-dimensional Lagrangian strain tensors quantified magnitude of skin deformation. To illustrate, consider neighboring markers with distance $\mathbf{ds_0}$ between them; $\mathbf{ds_0}$ has components $\mathrm{d}a_1$ and $\mathrm{d}a_2$ relative to a local orthogonal coordinate system. The two markers move to a new position during a response and the distance between them changes to the new value $\mathbf{ds}$. The change of distance between the two markers $\mathbf{ds}^2 - \mathbf{ds_0}^2$ is an exact measure of deformation in the two-dimensional plane of observation and may be written in the form of Lagrangian strain components (E_{11}, E_{12} and E_{22}) as follows [for derivation, see Fung (Fung, 1994), pp. 116–117]:

$$\mathbf{ds}^2 - \mathbf{ds_0}^2 = E_{11}\mathrm{d}a_1^2 + E_{22}\mathrm{d}a_2^2 + 2E_{12}\mathrm{d}a_1\mathrm{d}a_2 \qquad (1)$$

where E_{11}, E_{12} and E_{22} are non-dimensional quantities (length^2/length^2) that indicate local degree of two-dimensional stretch/compression and shear. They are readily computed by selection of a triad of markers [for further details, see e.g. Simon and Schmid-Schönbein (Simon and Schmid-Schönbein, 1990)].

E_{11}, E_{12} and E_{22} vary from instant to instant during the movement of markers, but eventually return to zero. Positions of the markers over frames 5–35 determined the coordinates before stimulation. The strains do not depend on translational displacement of markers (e.g. from head movement), but only deformation. E_{11} and E_{22} are normal strain components, E_{12} is the shear strain component.

The numerical values of E_{11}, E_{12} and E_{22} depend on choice of coordinates. In order to achieve maximum sensitivity to detect deformation, we computed the principal strains (Fung, 1994) as a measure for the maximum (and minimum) strain E_1 and E_2 in the area of the triads by solution of an eigenvalue problem for E_{11}, E_{12} and E_{22} (Simon and Schmid-Schönbein, 1990). Since principal strains E_1 and E_2 may be positive or negative, depending on the position of the markers, we computed an optimally sensitive measure of strain, $E_{\max}$, as

$$E_{max}^2 = E_1^2 + E_2^2$$

E_{max} was computed for every frame during a response.

Statistical analysis

Each triad of markers had its corresponding time-varying values of E_{max}. Triads of interest included those five to seven that formed triangles with bases on the bridge of the nose. Markers on the bridge remained relatively stationary during responses as the third marker of a triad moved. Not surprisingly, some triads showed more activity than others, but these varied somewhat from subject to subject depending upon local morphology. Analysis had as one outcome selection of responsive triads. Each subject had at least three.

The index d' from signal detection theory expressed the ability of E_{max} to resolve the differences among concentrations (Macmillan and Creelman, 1991). Calculation entailed: (i) log-transformation of E_{max} to approximate normal distributions; (ii) during each second, subtraction of mean log E_{max} for stimulation at 0 p.p.m. from mean log E_{max} for stimulation at >0 p.p.m.; and (iii) division of the differences by the average of the standard deviations of log E_{max} for 0 p.p.m. and that for each test concentration (see Appendix). In short, d' represented the difference, in units of standard deviation, between log E_{max} at baseline and log E_{max} associated with a given test concentration.

A matrix of d'-values for time, before and after the triggering signal, by concentration for each triad of interest provided the information to decide, for each subject, which three triads gave the best resolution between stimulus and blank. Values of d' averaged across the three most responsive triads per subject at each concentration and time became the information for further analysis.

Results

Figure 3 illustrates how E_{max} varied frame by frame for an individual subject. At the lower concentrations, deformation of the skin began during the second second after onset (frame 36) of the 3 s stimulus, reached a maximum, then declined. At the middle and upper concentrations, deformation increased throughout the 5 s period of taping after onset of the stimulus.

Figure 4 depicts how d' varied with concentration and time. Analysis of variance (ANOVA), within-subjects design, with six levels of time (0, 1, 2, 3, 4 and 5 s after onset of stimulus) and five levels of concentration uncovered significant effects of time [$F(5,45) = 7.31$, $P < 0.0001$], concentration [$F(4,36) = 5.50$, $P < 0.002$] and of the interaction time-by-concentration [$F(20,180) = 3.81$, $P < 0.0001$]. (One subject did not receive 4.3 log p.p.m. over the five trials because she found it too aversive, so the ANOVA included the results of just 10 subjects.)

As Figure 4 shows, the response began rather minimally during the first second, then increased sharply from the first to the second. Tests of significance of d' at individual time-points and concentrations versus baseline established reliability in the response by the second second. A routine computed the 95% confidence interval around d' in each of 30 cells (e.g. 3.6 log p.p.m. at 1 s versus 0 log p.p.m. at 1 s). Only five failed to lie outside their respective intervals: three concentrations at 0 s and two at 1 s. By 2 s, all concentrations had evoked responses significantly different from baseline (see Table 1). The response nevertheless continued to grow. For three of the five concentrations, the response reached its peak in the fourth second and for the other two it rose into the fifth.

The index d' incorporates both magnitude and variability of the measurements of strain. In this respect, d' behaves in the manner of a z-score and may be compared with results on detection (localization) of pungency, as shown in Figure 1. In the classical detection experiment, an observer must decide whether the sensory event on a trial came from a distribution of noise or a distribution of noise + signal. In the present experiment, a hypothetical observer can decide whether a given log E_{max} came from the distribution of noise, i.e. values of log E_{max} from presentations of 0 p.p.m., or from the distribution of noise + signal. From the following relationship, one can calculate the probability that an unbiased observer would be correct, e.g. respond 'blank' to 0 p.p.m. or 'stimulus' to a concentration >0 p.p.m.:

$$P(\text{correct}) = Z_{inv}(d'/2),$$

where Z_{inv} represents the inverse of the normal deviate transform [equation derived from equation (1.12) in Macmillan and Creelman (Macmillan and Creelman, 1991)]. Figure 5 shows a function for performance based upon d' in the fifth second of the response. Each data point comes from transformation of d' into proportion correct by subject and concentration, then averaging across subjects. It indicates that the observer would be correct 50% of the time, where chance equals 0%, at the concentration 3.96 log p.p.m.

Before the fifth second, the observer would require higher concentrations to achieve 50% correct. The 50% point can be viewed as the equivalent of a threshold that uses log E_{max} rather than the sensory observation to make the decision. The calculated threshold, so based, appears in Table 2. In the first second, the concentration necessary for 50% correct would be 5.6 log p.p.m., whereas in the second it would be 5.0 log p.p.m. and so on, down to 4.0 log p.p.m. (rounded).

Figure 5 also shows the psychometric function for nasal localization of ethyl acetate, repeated from Figure 1. The threshold in that study, where subjects sniffed for 2–3 s, was 3.94 log p.p.m. That is, the orbital response measured by strain had virtually identical sensitivity to chemesthetic perception. Since the slopes of the two functions differ, however, it could appear that the motor response has higher sensitivity below the 50% threshold and less sensitivity above

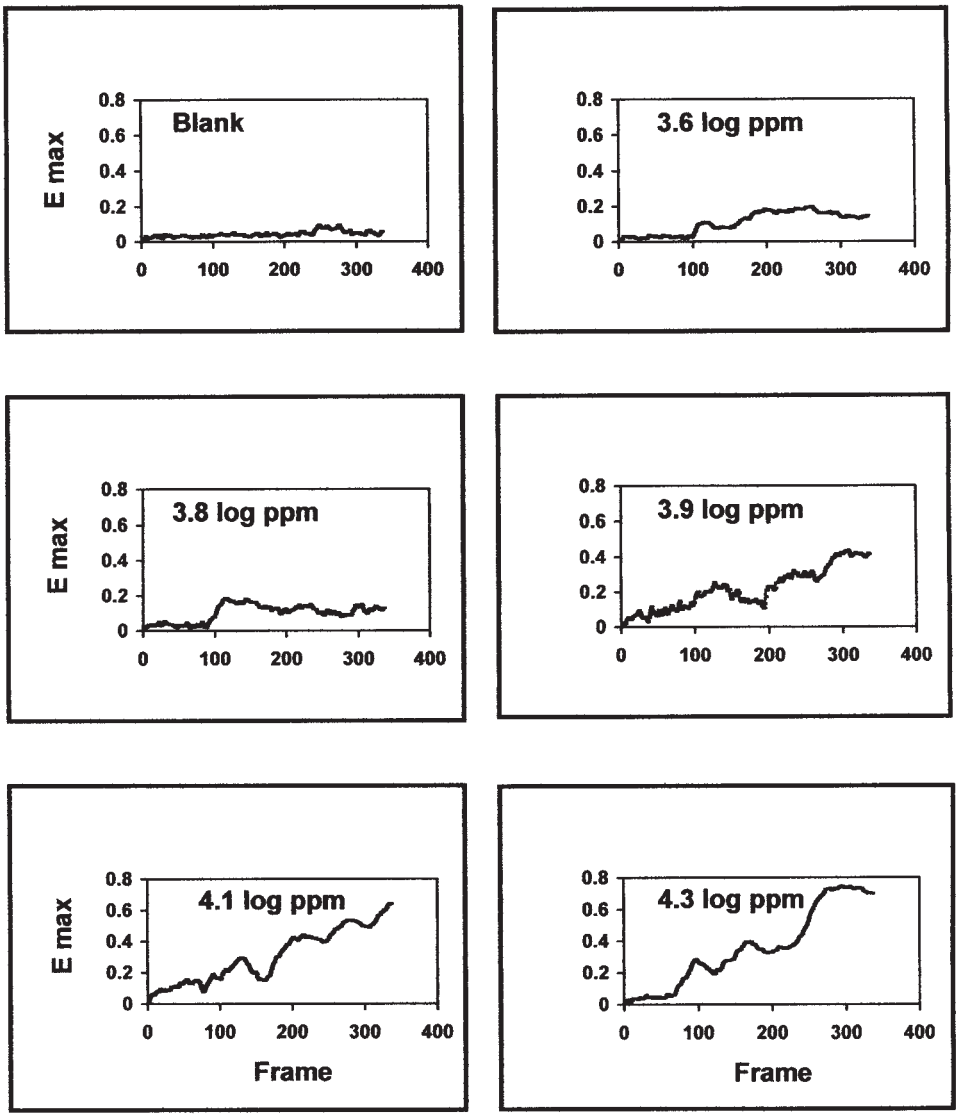

Figure 3 Showing how E_{max}, averaged across replicate presentations within a session, varied with frame for an individual subject.

it. More likely than not, this difference reflects how well the two measuring techniques captured the relative variances of the underlying sensory distributions. As Table 2 indicates, the slope of the function based upon the motor response increased second by second, showing that the signal-to-noise ratio increased over time and it could possibly have increased even more after 5 s. Collection of more data per subject would probably yield higher slopes throughout. The standard deviations of the two measures at a proportion correct of 0.50 were 0.1 and 0.3 for the psychophysical and orbital responses, respectively.

Discussion

The results confirm the suspicion, first raised upon monitoring of the face during studies of the apneic response, that contraction of the orbicularis oculi changes in concentration-dependent fashion with pungent chemesthetic stimulation. Other muscles also contract along with the orbicularis oculi, but fortunately the action of this one seems adequate to provide a viable objective index. Such an index was initially desired in part because the odor of pungent volatile organic compounds (VOCs) made it difficult to obtain unbiased measures of their chemesthetic potency in subjects with normal olfaction. For this reason, research on structure–activity relationships for chemesthesis in this laboratory resorted to the study of persons with anosmia (Cometto-Muñiz and Cain, 1990, 1991, 1993; Cometto-Muñiz *et al.*, 1998a,b). The situation changed as the technique based on localization proved its usefulness (Cometto-Muñiz and Cain, 1998). Nevertheless, the need to stimulate one nostril at a time in the localization procedure has limitations, particularly with respect to ecological validity. Furthermore, studies of threshold, whether for

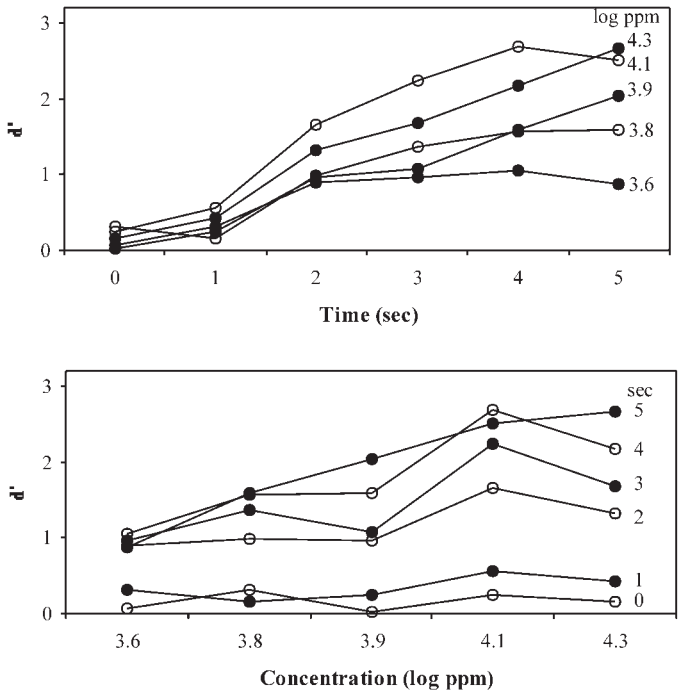

Figure 4 Showing how *d*′, based upon the magnitude and variability of maximum strain, varied with both concentration and time from the beginning of stimulation with ethyl acetate. Values at 0 s represent the average from images captured before the triggering signal, values at 1 s represent the average from images captured during the first second after the triggering signal, values at 2 s represent the average from images captured during the second second and so on, out to 5 s.

Table 1 *d*′, or difference of E_{max} from baseline in units of SD[a]

Time after onset (s)	Stimulus concentration (log p.p.m. v/v)				+ +
	3.6	3.8	3.9	4.1	4.3
0	**0.08**	0.31	**0.02**	0.25	**0.17**
1	0.32	**0.15**	**0.25**	0.55	0.43
2	0.90	0.98	0.97	1.67	1.31
3	0.95	1.35	1.07	2.24	1.68
4	1.06	1.56	1.59	2.69	2.16
5	0.87	1.58	2.05	2.52	2.65

[a]For values in bold type, 95% confidence interval of the mean includes zero.

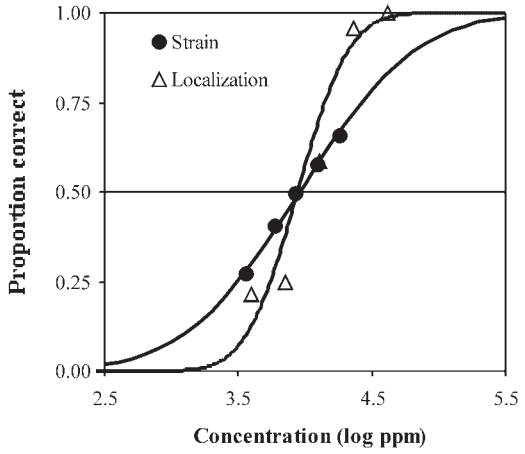

Figure 5 Psychometric functions for localization of ethyl acetate, as per Figure 1 and for detection of the stimulus via strain. The curves are best-fit cumulative Gaussian functions.

Table 2 Summary of linear fits to proportion correct (*z* units) based on strain versus log p.p.m.

Time (s)	Slope	r^2	Calculated threshold (log p.p.m.)	Multiple of localization threshold	Proportion of subjects who reached threshold[a]
1	0.65	0.40	5.6	46.3	0.00
2	0.44	0.47	5.0	11.6	0.36
3	0.78	0.69	4.3	2.3	0.55
4	1.00	0.97	4.1	1.5	0.64
5	1.45	0.99	4.0 (rounded)	1.0 (rounded)	0.82

[a]Proportion of subjects whose functions exceeded and stayed above 50% ($z = 0$), chance corrected, at or before 4.3 log p.p.m. All subjects reached localization threshold by 4.3 log p.p.m.

detection or for localization, have limitations based upon how long they take in testing, as the following illustrates.

Duration of an exposure plays an extremely important but poorly studied role in chemesthetic sensitivity. The thresholds measured and modeled in a quantitative structure–activity relationship (QSAR), a linear free-energy relationship, by Abraham, Cometto-Muñiz and associates (Abraham *et al.*, 1996, 1998a–c; Cometto-Muñiz *et al.*, 1998a) may represent chemesthesis at less than optimal potency in the sense that stimuli presented longer than the 2–3 s of a sniff may give lower, perhaps much lower thresholds. Indeed, chemesthetic potency may grow over minutes or even longer durations (Cain *et al.*, 1986). One can seek to measure thresholds over such exposures, but only with formidable expenditure of work. A technique that tracks a motor response at exposures of peri-threshold concentrations could accelerate the accumulation of information regarding how duration of exposure affects sensitivity by as much as an order of magnitude. Since the QSAR pivots on transport of molecules to a receptor biophase, it can readily incorporate time as a parameter. This situation illustrates just one application of several, but a pressing one (Cain and Cometto-Muñiz, 1995).

At this early stage, we cannot assert that the response of the orbicularis oculi will occur at the threshold for detection of all materials and all conditions of exposure. The correspondence found here occurred between two different groups tested under different regimes, but there is no reason

to believe that these two experiments should not have yielded the same answer either. As research goes forward, it should examine other materials, including some with unpleasant odors to insure that the response will have only chemesthetic determinants. W.S. Cain *et al*. (submitted for publication) studied various esters (acetates, propionates and butyrates) for their potency to evoke nasal pungency. The thresholds across these compounds correlated 0.99 with predictions of Abraham *et al*. (Abraham *et al*., 1998a). Furthermore, the thresholds correlated 0.99 with criterion amplitudes of the negative mucosal potential evoked by the same vapor delivery device and stimulating techniques used here. However, the strongest test for the correspondence between detection via conscious perception and via the motor response would come from trials where subjects seek to localize the nostril during measurement of the motor response.

Why does the response to stimulation of the nose occur in an orbital muscle? What would the orbital response mean if obtained in ambient exposures that could stimulate both the nose and the eye? The principal branch of the trigeminal nerve that endows the nose with chemesthesis, the ciliary branch, also innervates the eye. From an adaptive standpoint, that branch could play a protective role for both the nose and the eyes, for a noxious vapor that has access to the one site will have it to the other as well. Direct comparisons indicate that, despite the differences in their tissues, the eyes and nose have very similar, though perhaps not identical, chemesthetic sensitivity (Cometto-Muñiz and Cain, 1995, 1998). The QSAR that predicts nasal pungency bears substantial resemblance to that for the eye (Abraham *et al*., 1998b,c). The vapor delivery device used in the present study could help to settle the question of whether any differences might come from a factor such as flow rate of delivery to the respective organs and could establish whether the orbital response expresses itself similarly from nasal and ocular stimulation. For that effort, taping should, *inter alia*, go on longer than the 5 s employed here.

Our previous efforts, only modestly successful, to quantify the response via ratings of facial action highlight how much information the measure of maximum strain captured. As research goes forward to other chemesthetic agents such as other esters, it needs also to examine properties of the measurement of strain in greater detail. In Figure 4, the index based upon the scalar properties of $E_{\max}$ seems to have reached a maximum at or below the highest concentration. This may or may not reflect maximum deformation based on the properties of muscle. Further experimentation will tell.

Acknowledgements

Supported by grant 5 R01 DC 00284 from the National Institute on Deafness and Other Communication Disorders, National Institutes of Health. We thank Drs Roland Schmidt for technical assistance and J. Enrique Cometto-Muñiz for comments on the manuscript.

References

Abraham, M.H., Andonian-Haftvan, J., Cometto-Muñiz, J.E. and **Cain, W.S.** (1996) *An analysis of nasal irritation thresholds using a new solvation equation*. Fundam. Appl. Toxicol., 31, 71–76.

Abraham, M.H., Kumarsingh, K., Cometto-Muñiz, J.E. and **Cain, W.S.** (1998a) *An algorithm for nasal pungency thresholds in man*. Arch. Toxicol., 72, 227–232.

Abraham, M. H., Kumarsingh, R., Cometto-Muñiz, J.E. and **Cain, W.S.** (1998b) *A quantitative structure–activity relationship (QSAR) for a Draize eye irritation database*. Toxicol. In Vitro, 12, 201–207.

Abraham, M.H., Kumarsingh, R., Cometto-Muñiz, J.E. and **Cain, W.S.** (1998c) *Draize eye scores and eye irritation thresholds in man can be combined into one quantitative structure–activity relationship*. Toxicol. In Vitro, 12, 403–408.

Cain, W.S. and **Cometto-Muñiz, J.E.** (1995) *Irritation and odor as indicators of indoor pollution*. In Seltzer, R. (ed.), Occupational Medicine: State of the Art Reviews, Vol. 10. Hanley & Belfus, Philadelphia, PA, pp. 1–13.

Cain, W.S., See, L.-C. and **Tosun T.** (1986) *Irritation and odor from formaldehyde: chamber studies*. In IAQ '86: Managing Indoor Air for Health and Energy Conservation. American Society of Heating, Refrigerating and Air-conditioning Engineers, Atlanta, GA, pp. 126–137.

Cometto-Muñiz, J.E. and **Cain, W.S.** (1982) *Perception of nasal pungency in smokers and nonsmokers*. Physiol. Behav., 29, 727–731.

Cometto-Muñiz, J.E. and **Cain, W.S.** (1984) *Temporal integration of pungency*. Chem. Senses, 8, 315–327.

Cometto-Muñiz, J.E. and **Cain, W.S.** (1990) *Thresholds for odor and nasal pungency*. Physiol. Behav., 48, 719–725.

Cometto-Muñiz, J.E. and **Cain, W.S.** (1991) *Nasal pungency, odor and eye irritation thresholds for homologous acetates*. Pharmacol. Biochem. Behav., 39, 983–989.

Cometto-Muñiz, J.E. and **Cain, W.S.** (1993) *Efficacy of volatile organic compounds in evoking nasal pungency and odor*. Arch. Environ. Health, 48, 309–314.

Cometto-Muñiz, J.E. and **Cain, W.S.** (1995) *Relative sensitivity of the ocular trigeminal, nasal trigeminal, and olfactory systems to airborne substances*. Chem. Senses, 20, 191–198.

Cometto-Muñiz, J.E. and **Cain, W.S.** (1998) *Trigeminal and olfactory sensitivity: comparison of modalities and methods of measurement*. Int. Arch. Occup. Environ. Health, 71, 105–110.

Cometto-Muñiz, J.E., Cain, W.S. and **Abraham, M.H.** (1998a) *Nasal pungency and odor of homologous aldehydes and carboxylic acids*. Exp. Brain Res., 118, 180–188.

Cometto-Muñiz, J.E., Cain, W.S., Abraham, M.H. and **Kumarsingh, R.** (1998b) *Trigeminal and olfactory chemosensory impact of selected terpenes*. Pharmacol. Biochem. Behav., 60, 765–770.

Dunn, J.D., Cometto-Muñiz, J.E. and **Cain, W.S.** (1982) *Nasal reflexes: reduced sensitivity to CO_2 irritation in cigarette smokers*. J. Appl. Toxicol., 2, 176–178.

Ekman, P. and **Friesen, W.V.** (1975) Unmasking the Face: A Guide To Recognizing Emotions from Facial Clues. Prentice-Hall, Englewood Cliffs, NJ.

Ekman, P. and **Rosenberg, E.L.** (eds) (1997) What the Face Reveals: Basic and Applied Studies of Spontaneous Expression Using the Facial Action Coding System (FACS). Oxford University Press, New York.

Fung, Y.C. (1994) A First Course in Continuum Mechanics, 3rd edn. Prentice-Hall, Englewood Cliffs, NJ.

Garcia-Medina, M.R. and **Cain, W.S.** (1982) *Bilateral integration in the common chemical sense*. Physiol. Behav., 29, 349–353.

Kobal, G. (1985) *Pain-related electrical potentials of the human nasal mucosa elicited by chemical stimulation*. Pain, 22, 151–163.

Kobal, G. and **Hummel, C.** (1988) *Cerebral chemosensory evoked potentials elicited by chemical stimulation of the human olfactory and respiratory nasal mucosa*. Electroencephalogr. Clin. Neurophysiol., 71, 241–250.

MacMillan, N.A. and **Creelman, D.C.** (1991) Detection Theory: A User's Guide. Cambridge University Press, Cambridge.

Mazhari, R., Omens, J.H., Waldman, L.K. and **McCulloch, A.D.** (1998) *Regional myocardial perfusion and mechanics: a model-based method of analysis*. Ann. Biomed. Engng, 26, 743–755.

McCulloch, A.D., Sung, D., Wilson, J.M., Pavelec, R.S. and **Omens, J.H.** (1998) *Flow–function relations during graded coronary occlusions in the dog: effects of transmural location and segment orientation*. Cardiovasc. Res., 37, 636–645.

Shusterman, D.J. and **Balmes, J.R.** (1997) *A comparison of two methods for determining nasal irritant sensitivity*. Am. J. Rhinol., 11, 379–386.

Simon, S.I. and **Schmid-Schönbein, G.W.** (1990) *Cytoplasmic strains and strain rates in motile polymorphonuclear leukocytes*. Biophys. J., 58, 319–332.

Stevens, J.C. and **Cain, W.S.** (l986) *Aging and the perception of nasal irritation*. Physiol. Behav., 37, 323–328.

Widdicome, J.G. (1961) *Respiratory reflexes in man and other mammalian species*. Clin. Sci., 21, 163–171.

Accepted June 21, 2001

Appendix

The index d' assumes underlying distributions to be normal with equal variance. Analysis of receiver operating characteristic (ROC) curves can reveal violations of assumptions (Macmillan and Creelman, 1991). If data satisfy both assumptions, ROC curves in normal deviate coordinates are linear (normal distributions) with unit slope (equal variance). Normal deviate ROC curves for 33 conditions (three selected randomly from each subject) had an average Pearson's r of 0.96 (SD = 0.04) and slope of 1.14 (0.34). The good linear fits and slopes close to one suggest that the data came close to satisfying the assumptions on average.

To investigate the matter further, we computed two indexes of sensitivity based on areas under ROC curves for the sample of 33 conditions. Computation of one index entailed: (i) connecting the points of ROC curves through linear interpolation and (ii) computing the area under the resulting curves. Computation of the other index entailed integration of ROC curves corresponding to values of d' (calculated as described in the text) assuming normal underlying distributions with equal variance. The first index, which did not assume normal distributions with equal variance, correlated strongly (Pearson's $r = 0.98$) with the second, which did make these assumptions.